JRMP Journal of Radiopharmaceuticals and Molecular Probes Vol. 5, No.2, 2019
J Radiopharm Mol Prob 2019;5(2): 101-112
ISSN 2384-1583(Print) / ISSN 2508-3848(Online)

ORIGINAL ARTICLE

https://doi.org/10.22643/JRMP.2019.5.2.101

Comparative study of 2-nitroimidazole-fluorophore-conjugated derivatives with pimonidazole for imaging tumor hypoxia

Sudhakara Reddy Seelam [a-c], Mi Kyung Hong [a,b], Yun-Sang Lee [a,b], Jae Min Jeong [a-c*]

[a] Department of Nuclear Medicine, Institute of Radiation Medicine, Seoul National University College of Medicine, Seoul, Republic of Korea
[b] Cancer Research Institute, Seoul National University College of Medicine, Seoul, Republic of Korea
[c] Department of Radiation Applied Life Science, Seoul National University College of Medicine, Seoul, South Korea

ABSTRACT

Herein, 2-nitroimidazole-fluorophore conjugates were synthesized by linking 2-nitroimidazole and FITC or RITC via thiourea bonds. The prepared derivatives were stable for 2 h in Dulbecco's modified Eagle's medium (DMEM) at 37 °C. The novel conjugates were studied for their in vitro uptake under hypoxic conditions using U87MG and CT-26 cell lines, showing significantly higher uptakes in hypoxic than normoxic cells. Immunohistochemical analysis confirmed hypoxia in U87MG and CT-26 xenografted tumor tissues. Moreover, the prepared conjugates were evaluated by in vivo experiments after intravenous injection in U87MG and CT-26 xenografted mice. Hypoxia was confirmed by immunohistochemistry of the prepared derivatives with co-injected pimonidazole. Confocal microscopy of the prepared derivatives showed strong fluorescence in hypoxic tumor tissues correlated with the pimonidazole distribution. This suggested that the 2-nitroimidazole-fluorophore conjugates are promising optical imaging probes for tumor hypoxia and are promising substitutes for pimonidazole immunohistochemistry, which requires a multi-step procedure of incubation involving antibody, second antibody, dye, hydrogen peroxide, and multiple washing steps.

Key Word: FITC, RITC, immunohistochemistry, hypoxia, 2-nitroimidazole-FITC, and 2-nitroimidazole-RITC

Introduction

Radiolabeled nitroimidazole derivatives have been successfully applied for imaging hypoxia in animal models and humans. During this process, the nitroimidazole residue is reduced to reactive chemical species that bind to intracellular components in the absence of sufficient oxygen *(1-5)*.

Fluorescence-based detection techniques are commonly used for visualizing cellular processes and tumors as optical imaging has become an important tool. However, many potential choices are available in terms of fluorophores. Optical imaging is unique in its ability to be activated in situ as opposed to radionuclide imaging *(6,7)*, and is safer and easier to perform than nuclear imaging and other modalities *(8)*. Fluorescence imaging exhibits unique signal amplification, potentially leading to the selective imaging of cancer with higher tumor to non-tumor ratios *(9)*. An optical probe should be resistant to biodegradation after cellular internalization because it affects signal durability. Fluorescein is a fluorophore commonly used in microscopy and contains reactive fluorescein isothiocyanate derivative

Received: December 12, 2019 / Revised: December 26, 2019 / Accepted: December 28, 2019

Correspnding Author : Jae Min Jeong, Ph.D Department of Nuclear Medicine, Seoul National University Hospital, 101 Daehangno Jongno-gu, Seoul 110-744, Korea E-mail: jmjng@snu.ac.kr Tel: +82-2-2072-3805 Fax: +82-2-745-7690

(FITC) to label and track biological molecules in various applications *(10) (11)*. Rhodamine-based fluorophores are extensively used as fluorescent labeling reagents owing to their improved photostability and biostability compared to other dyes *(12,13)* and good photophysical properties including long absorption and emission wavelengths in the visible region, excellent fluorescence quantum yields, and large absorption coefficients *(14,15)*.

The ability to image real time events using fluorescence has made optical imaging attractive for the study of cellular and molecular events *(16)* and to visualize events in vivo, particularly in tumors *(17)*. Because it is noninvasive, optical imaging is simpler and less expensive, allowing for the precise assessment of the location and size of a tumor, providing information regarding invasiveness in adjacent tissues *(18)*.

It is well-known that 4-nitroimidazoles derivatives exhibit lower electron affinity and single electron reduction potential (SERP), unlike 2-nitroimidazole derivatives, and therefore, 2-nitroimidazole can be more efficiently reduced and retained in hypoxic cells *(19,20)*. Several 2-nitroimidazole based hypoxia markers labeled with various radionuclides *(21)* including ^{18}F *(22-27)*, ^{68}Ga *(28,29) (30)*, ^{124}I *(31)*, and the non-nitro bioreductive complex [^{64}Cu] diacetyl-bis(N4-methylthiosemicarbazone ([^{64}Cu]-ATSM) *(32)*) have been used for positron emission tomography (PET) studies. Nitroimidazole derivatives conjugated with fluorophores, including 2-nitroimidazole-ICG conjugates *(33,34)*, tricarbocyanine-nitroimidazole conjugated hypoxia probes, such as GPU-167 *(35)*, GPU-311 *(36)*, and 2-nitroimidazole-ICG conjugate attached to carbon nanotubes *(37)* have been developed. These studies showed that the 2-nitroimidazole-indocyanine green (ICG) conjugate remained in the tumors for a significantly longer period than ICG *(33) (38)*. Azobenzene-based fluorophores for in vivo fluorescence imaging of acute ischemia hypoxia *(39,40)*, iridium complexes as phosphorescence probe for imaging hypoxic lesions *(41)*, and near-infrared polymer-nanoprobes for *in vivo* imaging of tumor hypoxia *(42)* have been developed.

Herein, fluorophore-based nitroimidazole derivatives, such as 1-(3',6'-dihydroxy-3-oxo-3H-spiro[isobenzofuran-1,9'-xanthene]-5-yl)-3-(2-(2-nitro-imidazolyl)ethyl) thiourea **(3)** and 2-(3,6-bis(diethylamino)-9H-xanthen-9-yl)-5-(3-(2-(2-nitroimidazolyl)ethyl)thioureido) benzoic acid **(4)** were prepared by conjugation of 2-(2-nitroimidazolyl)ethylamine hydrochloride with **1** and **2**, respectively. These derivatives were used for the imaging hypoxia in tumor bearing mice models of U87MG (human glioblastoma) and CT-26 (mouse colon cancer).

Materials and methods

1. General

Hypoxyprobe™-1 (pimonidazole hydrochloride, an exogenous hypoxia marker) was purchased from Hypoxyprobe (Burlington, MA, U.S.A.). Hoechst 33342 (a blood perfusion marker) was purchased from Life technologies (Seoul, Korea). All other chemicals were purchased from Sigma-Aldrich (St. Louis, MO, USA). The ^{1}H and ^{13}CNMR spectra were recorded using a Bruker Avance 600 FT NMR spectrometer (600 MHz for ^{1}H and 150 MHz for ^{13}C; Bruker Ltd., Germany). The chemical shifts (δ) were reported in ppm downfield from tetramethylsilane and multiplicities were indicated by s (singlet), d (doublet), t (triplet), m (multiplet), or br (broad). Electrospray ionization mass spectra (ESI-MS) were acquired in positive ion mode using a Waters ESI ion trap spectrometer (Milford, MA, USA). The samples were diluted 1 to 100 times with methanol and injected directly into the injection port. The data was reported in terms of *m/z* versus intensity. The high resolution mass spectra (HRMS) were acquired using an LTQ-Orbitrap Velos ion trap spectrometer (Thermo Scientific, France). The purities of the synthesized compounds were confirmed as >99% by analytical high performance

liquid chromatography (HPLC; supporting information) with RP18 (4.5 mm x 100 mm) columns from Waters Corporation (Milford, MA, USA). The solvent systems used were A (H_2O) and B (EtOH) at a flow rate of 1 mL/min for analytical HPLC. The absorbance was measured using a S-3100 UV-vis spectrophotometer from Scinco (Seoul, Republic of Korea). Fluorescence was measured using a VarioskanTM flash multi reader from Thermo Scientific (Varian Analytical Instruments, Walnut Creek, CA, U.S.A.). Adhesion microscope slides (76 x 26 x 1 mm) were purchased from Marienfiled (Lauda-Königshofen, Germany). A Leica CM1800 Cryostat (IMEB Inc, CA, U.S.A.) was used for sectioning the cells and a Leica TCS SP8 (Leica Microsystems Ltd., Seoul, Korea) was used for in vitro fluorescence microscopic imaging.

All animal experiments were performed after the approval of the Institutional Animal Care and Use Committee of the Biomedical Research Institute at Seoul National University Hospital (3520150085). This institute is fully accredited by the Association for Assessment and Accreditation of Laboratory Animal Care. In addition, the National Research Council guidelines for the care and use of laboratory animals (revised in 1996) were observed throughout the study.

2. Chemical synthesis

1-(3',6'-Dihydroxy-3-oxo-3H-spiro[isobenzofuran-1,9'-xanthene]-5-yl)-3-(2-(2-nitro-imidazolyl)ethyl) *thiourea (3).* To the stirred solution of fluorescein isothiocyanate isomer 1 (0.050 g, 0.128 mmol) in anhydrous N,N-dimethylformamide(DMF),2-(2-nitroimidazolyl) ethylamine hydrochloride (0.030 g, 0.192 mmol) and triethyl amine (TEA, 0.03 mL, 0.247 mmol) were added. The mixture was stirred at room temperature in the dark overnight under an argon atmosphere. The reaction mixture was evaporated to dry under reduced pressure. The residue was purified via silica gel column chromatography using CH_2Cl_2/MeOH (8:2; Rf = 0.5) as an eluent to afford a yellow solid (0.057 mg, 81.4%). After purification, the obtained product was injected into an analytical HPLC (0–75% B for 30 min; Rt = 12.6 min), showing a single peak. 1H NMR (DMSO): δ 10.61 (br, 1H, NH), 8.65 (br, 1H, NH), 8.15 (s, 1H), 7.62–7.61 (d, J = 7.17 Hz, 1H), 7.50 (s, 1H), 7.13–7.12 (m, J = 7.93 Hz, 2H), 6.66–6.65 (d, J = 8.68 Hz, 2H), 6.55 (s, 2H), 6.51–6.50 (d, J = 8.68 Hz, 2H), 4.59–4.57 (t, J = 4.91, 2H), 4.00 (br, 2H, OH), 3.35–3.33(t, J = 7.55 Hz, 2H); ^{13}C NMR (DMSO): δ 181.20, 168.95, 166.97, 150.21, 144.81, 140.75, 129.44, 128.43, 127.76, 110.50, 102.38, 102.27, 48.60, 45.66, 43.10; HRMS (ESI+), (M+1)+ calcd. for $C_{26}H_{20}N_5O_7S$, 546.1083; found, 546.1080.

2-(3,6-Bis(diethylamino)-9H-xanthen-9-yl)-5-(3-(2-(2-nitro-1H-imidazol-1-yl)ethyl)thioureido)benzoic acid *(4).* To the stirred solution of rhodamine B isothiocyanate (0.040 g, 0.074 mmol) in DMF, 2-(2-nitroimidazolyl) ethylamine hydrochloride (0.017 g, 0.108 mmol) and TEA (0.015 mg, 0.02 mL, 0.147 mmol) were added. The mixture was stirred at room temperature in the dark overnight under an argon atmosphere. The reaction mixture was evaporated to dry under reduced pressure and the residue was purified via silica gel column chromatography using CH_2Cl_2/MeOH (8:2; R_f = 0.6) as an eluent, affording a pink solid (0.041 mg, 80.3%). After purification, the obtained product was injected into an analytical HPLC (0–75% B for 30 min; Rt = 13.2 min), showing a single peak. ^{1}H NMR ($CDCl_3$): 7.87–7.85 (m, 1H), 7.42–7.40 (m, 2H), 7.06–7.04 (m, 2H), 6.42–6.23 (m, 6H), 4.61–4.59(t, J = 5.28 Hz, 2H), 3.70–3.68 (t, J = 5.28 Hz, 2H), 3.34–3.30 (q, J = 7.1 Hz, 8H), 1.16–1.14 (t, J = 7.1 Hz, 12H). ^{13}C NMR (150 MHz, $CDCl_3$): δ (ppm) = 180.76, 167.79, 153.55, 153.27, 148.67, 132.13, 131.34, 128.87, 127.84, 123.69, 122.62, 108.02, 105.68, 97.74, 80.54, 64.71, 55.53, 53.14, 44.31, 38.56, 28.07, 12.57. HRMS (ESI+), $(M+1)^+$ calcd. for $C_{34}H_{38}N_7O_5S$ 656.2650 ; found, 656.2653.

3.Optical properties and quantum efficiency of fluorescence

The optical properties, including absorbance and emission of **1, 2, 3**, and **4** were examined in PBS. The absorbance was measured using a S-3100 UV-vis spectrophotometer from Scinco (Seoul, Republic of Korea). Fluorescence was measured by VarioskanTM flash multi reader from Thermo Scientific (Varian Analytical Instruments, Walnut Creek, CA, USA). The quantum yields were measured according to previously described methods *(36)*. The fluorescence measurements were performed at 25 °C.

4. Optical stability

The optical stability was measured according to previously published methods *(31)*. Briefly, the optical stability of **1** and **2** as well as the prepared derivatives **3** and **4** were tested in a cell culture medium at 37 °C. The effect of protein on the molecular stability was monitored by adding **1, 2, 3,** and **4** to a Dulbecco's modified Eagle's medium (DMEM) medium, from Welgene Inc., Korea. DMEM was maintained with 10% fetal bovine serum from Gibco (Life Technologies, Grand Island, NY, USA). For spectroscopic measurements, **1, 2, 3,** and **4** were suspended in a cell culture medium and incubated in a spectroscopic grade cuvette for measurement after 10, 30, 60, 90, and 120 min in dark to mimic the stability of the compounds. The integrated fluorescence intensities of **1, 2, 3,** and **4** after 10, 30, 60, 90, and 120 min of incubation were measured.

5. *In vitro* fluorescence imaging

The in vitro cell uptake studies were performed using U87MG (human glioblastoma) and CT-26 (mouse colon cancer) cell lines. The U87MG cell line was maintained in a minimum essential medium (MEM) obtained from Gibco (Life Technologies, Grand Island, NY, USA) and CT-26 cell line was maintained in DMEM medium from Welgene Inc., Korea. Both media were maintained with 10% fetal bovine serum from Gibco (Life Technologies, Grand Island, NY, USA) and 1% antibiotic mixture (penicillin:streptomycin:amphotericin B = 10,000 IU:10 mg:25 μg in 1 mL, Mediatech Inc., Manassas, VA, USA) in a 5% CO_2 incubator at 37 °C. The cells (5 x 10^4 cells / 0.5 mL / well) were sub-cultured overnight in 8-well plates obtained from NalgenNunc (Naperville, IL, USA). Pre-incubation was subsequently performed under normoxic (5% CO_2 in air) or hypoxic (5% CO_2 in 95% N_2) conditions for 4 h, followed by incubation with 0.1 mg/mL **3** or **4** for 1 h. The wells were subsequently washed thrice with 1 mL DMEM with 1% FBS medium to remove unbound **3** or **4** from the cells. Further, 10 μL of the Prolong Gold antifade reagent with DAPI from Molecular Probes (Life Technologies, Grand Island, NY, USA) was added and covered with glassy cover slips. After drying, high resolution fluorescence imaging was performed to visualize **3** or **4** in each well using a Leica TCS SP8 confocal microscope. The excitation and emission channels were set to 488 and 518 nm, respectively, for FNI; while they were set to 570 and 595 nm for RNI; and 352 and 461 nm for DAPI; with a bandwidth of 40 to 50 nm. The images were obtained using the LAS AF Lite analysis software provided by the manufacturer.

6. Immunohistochemistry

The immunohistochemistry study was performed according to the previously published methods *(30)*. Hypoxyprobe™-1 (pimonidazole hydrochloride (60 mg/kg)) was diluted in 150 μL of PBS and intravenously injected into the CT-26 and U87MG xenografted mice (n=3 in each case). The mice were sacrificed 1.5 h post-injection and the tumor was isolated and directly frozen in liquid nitrogen until cryosectioning into 7 μm thin slices using a Leica CM1800 Cryostat (IMEB Inc., CA, USA). The sections were then stored at -80 °C prior to staining. The fixed tumor sections were washed with PBS containing 0.2% Brij 35 and exposed to 3% hydrogen peroxide for 5 min at room temperature to quench endogenous peroxidase activity. The sections were incubated with a protein-blocking agent for 5 min at room temperature to

minimize non-specific binding. The samples were then incubated for 60 min at room temperature with mouse monoclonal anti-pimonidazole antibody (MAb1) diluted in PBS and washed. The samples were incubated with a secondary biotinylated antibody (Vector Laboratories Inc., Burlingame, CA, USA), a biotin-streptavidin-peroxidase complex, and 3,3′-diaminobenzidine (DAB), imparting a clear brown color to the marker-antibody complex around the hypoxic cell nuclei. Between all steps of the staining procedure, the sections were rinsed thrice with PBS (0.2% Brij 35) for 2 min at 0 °C. Finally, the sections were mounted using CC/Mount from Sigma/Aldrich (St. Louis, MO, U.S.A.). The cells and histological sections were viewed with a microscope (Olympus America Inc., Melville, NY, USA) to investigate their staining and hypoxia status.

7. *Ex-vivo* fluorescence imaging

The prepared derivatives **3** and **4** for tumor targeting in vivo were tested using U87MG (Human glioblastoma) in nude mouse and CT-26 (mouse colon cancer) in BALB/c mouse. Each mouse was injected subcutaneously with 2 x 10^5/0.1 mL U87MG or CT-26 cells on the right shoulder (n=3 in each case). After 2 weeks, the drug formulations of **3** (30 mg / kg) and **4** (30 mg / kg) were co-injected with pimonidazole hydrochloride (60 mg / kg) in 150 μL of PBS intravenously into each xenografted mouse. Hoechst 33342 (10 mg / kg) was injected 5 min prior to mice sacrifice. The mice were sacrificed 1.5 min post-injection and the tumor or tissue specimens were collected and directly frozen in liquid nitrogen until cryosectioning into 7 μm thin slices using a Leica CM1800 cryostat (IMEB Inc., CA, USA). The sections were then stored at -80 °C prior to staining. The fixed tumor sections were washed with PBS containing 0.2% Brij 35 and exposed to 3% hydrogen peroxide for 5 min at room temperature to quench the endogenous peroxidase activity. The sections were incubated with a protein-blocking agent for 5 min at room temperature to minimize non-specific binding. The samples were incubated for 60 min at room temperature with mouse monoclonal anti-pimonidazole antibody (MAb1) diluted in PBS and washed. The samples were incubated with a secondary biotinylated antibody (Vector Laboratories Inc., Burlingame, CA, USA), a biotin-streptavidin-peroxidase complex, and with DAB. Between all steps of the staining procedure, the sections were rinsed thrice with PBS (0.2% Brij 35) for 2 min at 0 °C. Finally, the sections were mounted using CC/Mount from Sigma-Aldrich (St. Louis, MO, USA). High resolution fluorescence imaging was performed to visualize **3** or **4** in the tumor areas using an Olympus DP50 fluorescence microscope (Olympus America Inc., Melville, NY, USA) equipped with the following filters: excitation wavelength 350 to 600 nm, emission wavelength 460 to 650 nm. This instrument provided a scan resolution ranging from 21 to 339 μm. The fluorescence images obtained herein were acquired at 100 μm. The excitation and emission wavelengths were 488 and 518 nm, respectively, for green; 570 and 595 nm for red; and 352 and 461 nm for the blue filter.

Results and discussion

1. Chemistry

The nitroimidazole residue 2-(2-nitroimidazolyl) ethylamine hydrochloride was synthesized according to the previously published methods(28) (29). To synthesize **3** and **4**, FITC, 2-(2-nitroimidazolyl)ethylamine hydrochloride, and RITC, 2-(2-nitroimidazolyl)ethylamine were conjugated in DMF using TEA as a base (Scheme 1). Products formation during both reactions was monitored by electrospray ionization mass spectrometry in positive ion mode (MS/ESI^+). Products **3** and **4** were purified via silica gel column chromatography with yields of 81.4 and 80.3%, respectively. The chemical structures of the synthesized products were confirmed by NMR and mass

spectroscopy. The purities of the synthesized compounds were determined by analytical HPLC and were confirmed by a single peak appearance. The chemical synthesis of the prepared derivatives was easy and the final product yields were quantitative.

2. Absorption and fluorescence properties

The fluorophores 1, 2, and the 2-nitroimidazole conjugates of **3** and **4** were spectrally characterized using a UV-vis spectrophotometer and fluorescence spectrophotometer. The wavelength range of both spectrophotometers was 400–800 nm. The dyes were dissolved in PBS and the absorption and fluorescence spectra were recorded. The spectral properties of **1, 2, 3,** and **4** are shown in Table 1, with absorbance peaks at 493–558 nm and fluorescence peaks at 520–590 nm. Both the prepared derivatives **3** and **4** showed hypochromic effects in their absorption and emission spectra (supporting information Figure S6). The decreased absorption and emission maximum was likely owing to the addition of the nitroimidazole residue, which caused a structural difference in the prepared derivatives compared to original structures of **1** and **2**. Compounds **3** and **4** showed a hypochromic effect (blue shift) of 10 and 8 nm, respectively, in their absorption spectra (Table 1). However, no blue shift was observed in emission spectra of both derivatives. The prepared derivatives were stable up to 2 h in DMEM at 37 °C (Figure 2). These results confirmed that bleaching or spectral fluctuations of the dye conjugates during real-time in-vivo imaging were unlikely, where the **3** and **4** binding to the hypoxic cells were the main focus.

An important principle for efficient fluorescence imaging probes includes sufficient pharmacological properties, such as water solubility, low non-specific binding, rapid clearance of the free dye, and low toxicity with appropriate photophysical properties, such as excitation and emission maximum in the visible region between 400–700 nm, high quantum yield, as well as chemical and optical stability. The prepared derivatives **3** and **4** showed good aqueous

Table 1. Optical properties of **1, 2, 3,** and **4** in PBS at 25 °C

Compound	λabs (nm)	λem (nm)	Quantum Yield (ϕ)
1	493	520	0.75 (55)
2	558	590	0.59 (56)
3	483	520	0.69
4	550	590	0.52

Scheme 1. Syntheses of 3 and 4.

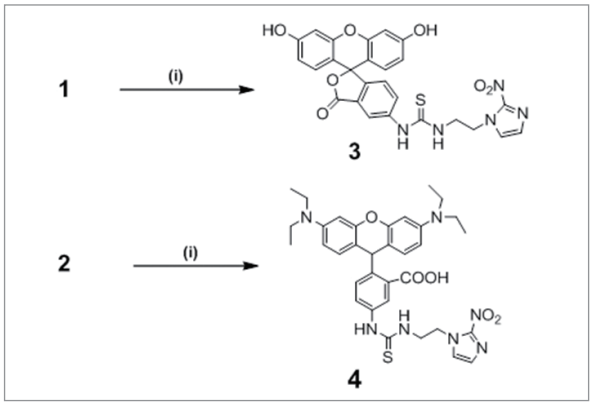

[a] Reagents and conditions: (i) 2-(2-nitroimidazolyl)ethylamine hydrochloride, triethylamine, and DMF, overnight.

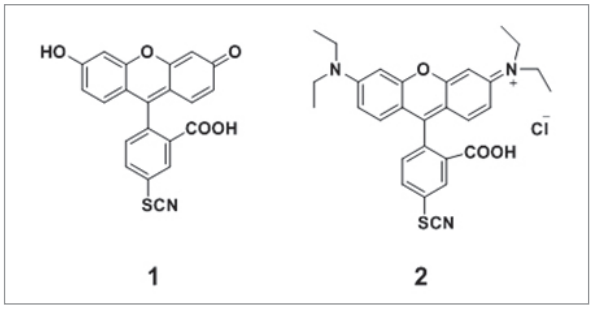

Figure 1. Structures of fluorescein isothiocyanate (**1**, FITC) and rhodamine B isothiocyanate (**2**, RITC).

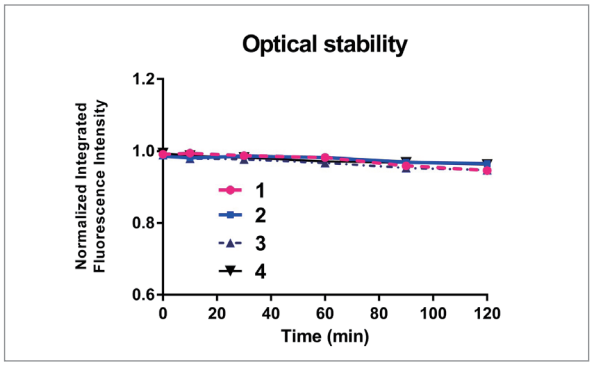

Figure 2. Optical Stability of the prepared 2-nitroimidazole derivatives **3** and **4** in the cell culture medium at 37 °C.

solubility and high stability for 2 h (Figure 2). These stability results confirmed the lack of significant bleaching or spectral fluctuations of the prepared conjugates under the current conditions.

3. *In vitro* fluorescence imaging

To evaluate the hypoxia selectivity of the prepared derivatives **3** and **4**, in vitro fluorescence imaging was performed using U87MG and CT-26 cancer cell lines (Figure 3). Prior to imaging, pre-incubation was performed for 4 h under normoxic or hypoxic conditions. Later, the cells were incubated with **3** and **4** separately under normoxic or hypoxic conditions for 1 h in fresh medium and washed with DMEM to remove unbound dye. The DAPI reagent was added to visualize the nuclei using a Leica TCS SP8 confocal microscope to confirm the uptake of the **3** and **4** in the hypoxic cells. The in vitro data revealed that the newly synthesized derivatives accumulated in tumor cells under hypoxic conditions, indicating that these compounds may bind to intracellular substances irreversibly and selectively retained in hypoxic cells. The results suggested that **3** and **4** may penetrate and bind to intracellular substances irreversibly in hypoxic cells to a larger extent than those in aerobic cells.

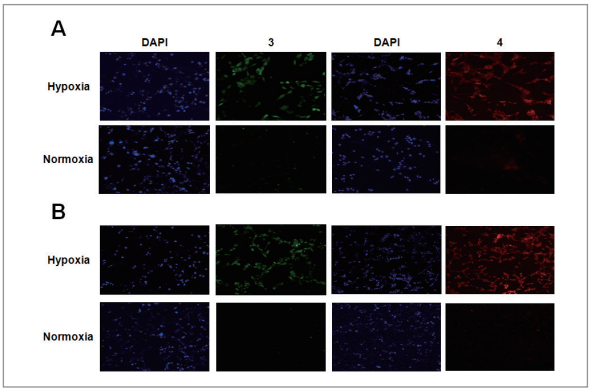

Figure 3. *In vivo* confocal microscopy images of the prepared derivatives **3** and **4** in A) U87MG; and B) CT-26 cancer cell lines (original magnification 100×). Green (3) and red staining (4) with the blue color indicating the presence of nuclei stained with DAPI. Original magnification 100×

4. Immunohistochemistry

Hypoxia in the U87MG and CT-26 xenografted tumor tissues was verified by immunohistochemical analysis. After injection of a standard exogenous bioreductive hypoxia marker, pimonidazole hydrochloride, into U87MG and CT-26 xenografted mice via the tail vein, the mice were sacrificed after 1.5 h. The tumors were dissected and cut into 7 μm slices at -20 °C and were processed using the antibody kit obtained from Hypoxyprobe. Immunohistochemical staining (brown) revealed the hypoxic areas (Figure 4).

Pimonidazole is the gold standard exogenous hypoxic marker for immunohistochemical studies of hypoxia in solid tumors. The binding of pimonidazole to cellular macromolecules increases considerably at oxygen concentrations of <10 mmHg and is believed to indicate chronic hypoxia *(43)*. However, the immunohistochemical (IHC) detection of hypoxia is particularly appealing because the hypoxic regions can be directly visualized in situ and compared with the underlying cellular architecture *(44)*. IHC detection of hypoxia in murine tissues can be problematic due to the presence of inherent normal mouse immunoglobulins because the primary monoclonal antibody (Mab) used to detect pimonidazole adducts in the proteins of hypoxic tissues is of mouse origin. Therefore, even when special blocking procedures were performed, immunostaining of mouse tissues with primary mouse antibodies produced extensive background staining that complicated the specific binding pattern of the primary antibody *(45)*. However, pimonidazole IHC analysis

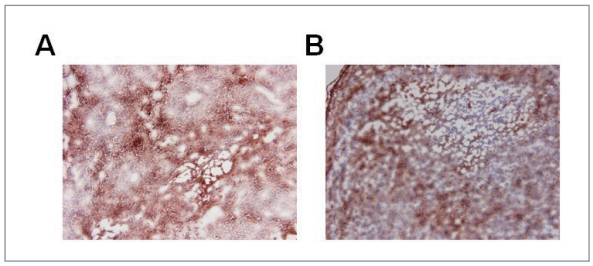

Figure 4. Immunohistochemical staining of A) U87MG; B) CT26 tumor xenografts to detect hypoxia. The tumor tissue was obtained from xenografted mice 1.5 h after intravenous injection of Hypoxyprobe™-1. The hypoxic lesions are shown in brown. (A) and (B) 100× magnification images

requires a long incubation with the first antibody, second antibody, dye, hydrogen peroxide, and the multiple washing steps. Therefore, pimonidazole-based IHC is cumbersome, tedious, and difficult.

5. *Ex-vivo* fluorescence imaging

Next, **3** and **4** were evaluated by ex-vivo fluorescence imaging experiments of the xenografts of CT-26 and U87MG mice. Compounds 3 and 4 were co-injected with pimonidazole intravenously into each xenografted mouse (Figure 5). Hoechst 33342 was injected 5 min prior to mice sacrifice, which occurred 1.5 h post-injection. The tumor specimens were collected, cut into 7 μm thick slices and processed with an antibody kit from Hypoxyprobe to visualize Hypoxyprobe™-1. High resolution fluorescence imaging was performed to confirm the presence of the **3** or **4** in the tumors using a fluorescence microscope. Higher **3** and **4** accumulation in hypoxic tumor tissues were observed compared to the surrounding normal tissues. With evidence for hypoxia, a strong and significant correlation was observed between **3, 4** and the pimonidazole (Figure 5). Compounds **3** and **4** as well as the pimonidazole stain was localized in most cases at a distance from a perfused (Hoechst) blood vessel. However, 3 and 4 were selectively observed in the hypoxia region, while some studies indicated that pimonidazole staining occurred in close proximity to the perfusion marker due to perfusion limited hypoxia *(22)*.

These observations suggested that the prepared derivatives **3** and **4** efficiently detected hypoxic regions in vivo, which was confirmed after ex-vivo fluorescence imaging. Assessment of the hypoxic fractions in tumors, which are regarded as adverse prognostic factors for tumor progression and indicators of the necessity for tumor-specific treatment, provides diagnostic and therapeutic advantages for various cancer treatments *(46)*.

2-Nitroimidazole-indocyanine green (ICG) and 2-nitroimidazole-tricarbocyanine conjugate were previously reported *(33,34) (35) (36)*. These studies

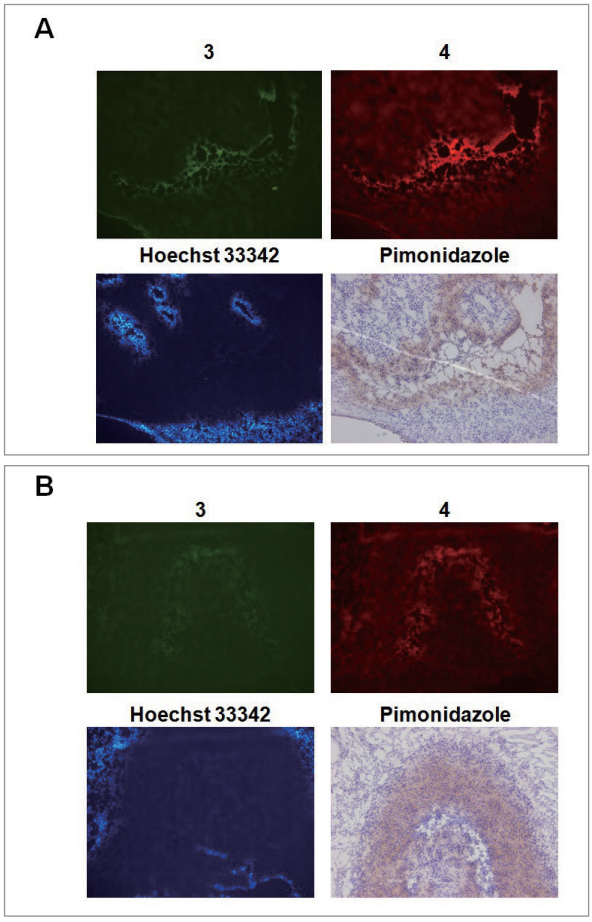

Figure 5. *Ex-vivo* fluorescence microscopic images (100×) of the prepared derivatives **3** and **4** co-injected with pimonidazole in A) U87MG; B) CT-26 xenografted mice intravenously 1.5 h post-injection. Green **(3)**, red **(4)**, blue (Hoest 33342), and brown staining (pimonidazole). Hypoxia was observed in **3, 4,** and pimonidazole staining and the nuclei were stained in blue.

proved that the ICG conjugate remained in the tumors for a significantly longer period than the ICG alone *(33) (38)*. However, hypoxia in tumors was confirmed using an anti-pimonidazole antibody stain after sacrifice, however, it was difficult to correlate the NIR fluorescence image with pimonidazole staining *(38)*. However, ICG is an FDA approved NIR fluorophore and is a blood pool agent that is not inherently specific for any tumor tissue, not making it ideal for oncologic image-guided surgery *(47)*. However, ICG is used for human subjects due to its low toxicity and high absorbance in the NIR spectrum. ICG use in molecular imaging probes may be limited because it loses fluorescence after protein binding. ICG is selectively distributed to the liver and excreted rapidly into the bile

because it becomes tightly bound to serum proteins *(48)*. Non-specific fluorescence was also possible with ICG upon binding to plasma proteins, with the protein-bound ICG emitting light at approximately 830 nm in the NIR *(49)* and is rapidly washed out from tumors in < 3 h *(38)*. 2-Nitroimidazole-tricarbocyanine conjugates, such as GPU-167 and GPU-311 are rapidly eliminated through the liver *(35) (36)*. A monoclonal anti-pimonidazole antibody, Mab1, was directly conjugated with FITC and used as a primary antibody reagent to overcome the extensive background staining. This facilitated the accurate and quantitative detection of hypoxia gradients in 4T1 mammary adenocarcinoma tumor bearing mice *(44)*.

For hypoxia targeting imaging, 2-nitroimidazole-based imaging agents served as an important exogenous markers because of their unique behavior in hypoxic environments owing to their high electron affinity (5) *(50)*. In particular, 2-nitroimidazole is reduced by an enzyme-mediated (nitro reductase) single electron reduction to form a free radical. After hypoxia-sensitive reduction of the nitro group to an amine, radiolabeled or fluorophore conjugated nitroimidazoles bind to intracellular proteins in the tumor (supporting information Figure S5) *(1)*. Therefore, the development of radiolabeled or fluorophore conjugated nitroimidazole derivatives for imaging of tumor hypoxia remains an active field of research to improve cancer therapy outcomes *(21,28,51,52)*.

The clinical importance of hypoxia PET imaging using agents, such as [^{18}F]fluoromisonidazole ([^{18}F]FMISO), [^{18}F]fluoroazomycin ([^{18}F]FAZA), 3-[^{18}F]fluoro-2-(4-((2-nitro-1H-imidazol-1-yl)methyl)-1H-1,2,3-triazol-1-yl)propan-1-ol ([^{18}F]HX4), [^{18}F]fluoroerythronitroimidazole ([^{18}F]FETNIM), and [^{64}Cu]diacetyl-bis(N4-methylthiosemicarbazone ([^{64}Cu]-ATSM) have been previously reviewed (structures provided in supporting information Figure S1) *(53)*. However, radionuclide imaging requires radioactive compounds, which exhibit intrinsically limited half-lives and expose the patient and practitioner to ionizing radiation. Therefore, these materials are subject to a variety of stringent safety regulations that limit their repeated use *(36)*. Fluorescence-based detection is a sensitive and quantitative method that is widely used in molecular biology and biochemistry for a variety of experimental, analytical, and quality control applications *(54)*.

Consequently, the design strategy of using nitroimidazole-fluorophore conjugates for fluorescence imaging of hypoxic tissue is promising for developing tumor hypoxia probes for ex-vivo fluorescence imaging. The ex-vivo fluorescence imaging of hypoxia tissue is straight-forward compared to pimonidazole IHC. However, further studies elucidate the time required for drug wash-out are needed to improve the nitroimidazole-fluorophore conjugates for application in vivo hypoxia imaging.

Conclusion

Fluorescent hypoxia probes, comprised of 2-nitroimidazole as a hypoxia marker, FITC, and RITC were developed for ex-vivo fluorescence imaging of tumor hypoxia. The chemical syntheses of **3** and **4** were easy and yields were quantitative. Compounds **3** and **4** showed absorbance and fluorescence peaks at 483 / 550 nm and 520 / 590 nm, respectively. The dye-conjugates showed a blue shift of 10 and 8 nm for **3** and **4**, respectively, in the absorption spectra compared to those of the standards **1** and **2**. The prepared derivatives were stable up to 2 h in cell culture medium at 37 °C. The newly synthesized probes, **3** and **4**, were trapped in tumor cells cultured under hypoxic conditions to a greater extent than that under hypoxic conditions. IHC staining of tumor hypoxia using HypoxyprobeTM-1 showed hypoxia lesions in the U87MG and CT-26 tumor xenograft tissue. In the *ex-vivo* fluorescence imaging, the regions of hypoxia in tumors in mice were clearly visualized and correlated with pimonidazole staining. The ex-vivo fluorescence imaging

of tumor hypoxia is easier and more straightforward than pimonidazole IHC. In conclusion, a novel fluorescence imaging procedure was developed herein for detecting regions of hypoxia in U87MG and CT-26 tumor bearing mice.

References

1. Nunn A, Linder K, Strauss HW. Nitroimidazoles and imaging hypoxia. *Eur J Nucl Med* 1995;22:265-280.
2. Rauth A, Melo T, Misra V. Bioreductive therapies: an overview of drugs and their mechanisms of action. *Int J Radiat Oncol Biol Phys* 1998;42:755-762.
3. Takasawa M, Moustafa RR, Baron J-C. Applications of nitroimidazole in vivo hypoxia imaging in ischemic stroke. *Stroke* 2008;39:1629-737.
4. Sorger D, Patt M, Kumar P, Wiebe LI, Barthel H, Seese A, Dannenberg C, Tannapfel A, Kluge R, Sabri O. [^{18}F] Fluoroazomycinarabinofuranoside (^{18}FAZA) and [^{18}F] fuoromisonidazole (^{18}FMISO): a comparative study of their selective uptake in hypoxic cells and PET imaging in experimental rat tumors. *Nucl Med Biol* 2003;30:317-326.
5. Kizaka-Kondoh S, Konse-Nagasawa H. Significance of nitroimidazole compounds and hypoxia-inducible factor-1 for imaging tumor hypoxia. *Ca Sci* 2009;100:1366-1373.
6. Urano Y. Sensitive and selective tumor imaging with novel and highly activatable fluorescence probes. *Anal Sci* 2008;24:51-53.
7. Weissleder R, Mahmood U. Molecular imaging. *Radiology* 2001;219:316-333.
8. Keereweer S, Kerrebijn JD, van Driel PB, Xie B, Kaijzel EL, Snoeks TJ, Que I, Hutteman M, van der Vorst JR, Mieog JS, Vahrmeijer AL, van de Velde CJ, Baatenburg de Jong RJ, Löwik CW. Optical image-guided surgery--where do we stand? *Mol Imaging Biol* 2011;13:199-207.
9. Choi HS, Gibbs SL, Lee JH, Kim SH, Ashitate Y, Liu F, Hyun H, Park G, Xie Y, Bae S, Henary M, Frangioni JV. Targeted zwitterionic near-infrared fluorophores for improved optical imaging. *Nat Biotech* 2013;31:148-153.
10. Schauenstein K, Schauenstein E, Wick G. Fluorescence properties of free and protein bound fluorescein dyes. I. Macrospectrofluorometric measurements. *J Histochem Cytochem* 1978;26:277-283.
11. Hawkins DM, Trache A, Ellis EA, Stevenson D, Holzenburg A, Meininger GA, Reddy SM. Quantification and confocal imaging of protein specific molecularly imprinted polymers. *Biomacromolecules* 2006;7:2560-2564.
12. Bremer C, Ntziachristos V, Weissleder R. Optical-based molecular imaging: contrast agents and potential medical applications. *Eur Radiol* 2003;13:231-243.
13. McCann TE, Kosaka N, Koide Y, Mitsunaga M, Choyke PL, Nagano T, Urano Y, Kobayashi H. Activatable optical imaging with a silica-rhodamine based near infrared (SiR700) fluorophore: a comparison with cyanine based dyes. *Bioconjug. Chem* 2011;22:2531-2538.
14. Lackowicz JR. Principles of fluorescence spectroscopy. Plenum Press,(New York, 1983) *Chapter* 1983;5:111-150.
15. Mei L, Xiang Y, Li N, Tong A. A new fluorescent probe of rhodamine B derivative for the detection of copper ion. *Talanta* 2007;72:1717-1722.
16. Massoud TF, Gambhir SS. Molecular imaging in living subjects: seeing fundamental biological processes in a new light. *Genes Dev* 2003;17:545-580.
17. Brindle K. New approaches for imaging tumour responses to treatment. *Nat Rev Ca* 2008;8:94-107.
18. Jager HR, Taylor MN, Theodossy T, Hopper C. MR imaging-guided interstitial photodynamic laser therapy for advanced head and neck tumors. *Am J Neuroradiol* 2005;26:1193-1200.
19. Chu T, Hu S, Wei B, Wang Y, Liu X, Wang X. Synthesis and biological results of the technetium-99m-labeled 4-nitroimidazole for imaging tumor hypoxia. *Bioorg Med Chem Lett* 2004;14:747-749.
20. Li Z, Zhang J, Jin Z, Zhang W, Zhang Y. Synthesis and

biodistribution of novel 99mTc labeled 4-nitroimidazole dithiocarbamate complexes as potential agents to target tumor hypoxia. *Med Chem Commun* 2015;6:1143-1148.

21. Hoigebazar L, Jeong JM. Hypoxia Imaging Agents Labeled with Positron Emitters. Theranostics, Gallium-68, and Other Radionuclides: *Springer*; 2013, p. 285-299.
22. Dubois LJ, Lieuwes NG, Janssen MH, Peeters WJ, Windhorst AD, Walsh JC, Kolb HC, Ollers MC, Bussink J, van Dongen GA, van der Kogel A, Lambin P. Preclinical evaluation and validation of [^{18}F] HX4, a promising hypoxia marker for PET imaging. *Proc Nat Acad Sci* 2011;108:14620-14625.
23. Halmos GB, Bruine de Bruin L, Langendijk JA, van der Laan BFAM, Pruim J, Steenbakkers RJHM. Head and neck tumor hypoxia imaging by ^{18}F-fluoroazomycin-arabinoside (^{18}F-FAZA)-PET: A Review. *Clin Nucl Med* 2014;39:44-48.
24. Hoigebazar L, Jeong JM, Lee Y-S, Hong MK, Kim YJ, Lee J-Y. Synthesis and evaluation of (AlF)-F-18-NODA-nitroimidazole derivatives and their feasibility study as hypoxia PET agents. *J Label Cmpd Radiopharm* 2011, 54:S493 (suppl).
25. Kumar P, Naimi E, McEwan AJ, Wiebe LI. Synthesis, radiofluorination, and hypoxia-selective studies of FRAZ: A configurational and positional analogue of the clinical hypoxia marker, [^{18}F]-FAZA. Bioorg Med Chem 2010;18:2255-2264.
26. Mahy P, Geets X, Lonneux M, Leveque P, Christian N, De Bast M, Gillart J, Labar D, Lee J, Grégoire V. Determination of tumour hypoxia with [^{18}F]EF3 in patients with head and neck tumours: a phase I study to assess the tracer pharmacokinetics, biodistribution and metabolism. *Eur J Nucl Med Mol Imaging* 2008;35:1282-1289.
27. Prekeges JL, Rasey JS, Grunbaum Z, Krohn KH. Reduction of fluoromisonidazole, a new imaging agent for hypoxia. *Biochem Pharmacol* 1991;42:2387-2395.
28. Hoigebazar L, Jeong JM, Choi SY, Choi JY, Shetty D, Lee Y-S, Lee DS, Chung JK, Lee MC, Chung YK. Synthesis and characterization of nitroimidazole derivatives for ^{68}Ga-labeling and testing in tumor xenografted mice. J *Med Chem* 2010;53:6378-6385.
29. Hoigebazar L, Jeong JM, Hong MK, Kim YJ, Lee JY, Shetty D, Lee YS, Lee DS, Chung JK, Lee MC. Synthesis of ^{68}Ga-labeled DOTA-nitroimidazole derivatives and their feasibilities as hypoxia imaging PET tracers. *Bioorg Med Chem* 2011;19:2176-2181.
30. Seelam SR, Lee JY, Lee Y-S, Hong MK, Kim YJ, Banka VK, Banka VK, Lee DS, Chung JK, Jeong JM. Development of 68Ga-labeled multivalent nitroimidazole derivatives for yypoxia imaging. *Bioorg Med Chem* 2015;23:7743-7750.
31. Reischl G, Dorow DS, Cullinane C, Katsifis A, Roselt P, Binns D, Hicks RJ. Imaging of tumor hypoxia with [^{124}I] IAZA in comparison with [^{18}F]FMISO and [^{18}F]FAZA--first small animal PET results. *J Pharm Pharm Sci* 2007;10:203-211.
32. Obata A, Kasamatsu S, Lewis JS, Furukawa T, Takamatsu S, Toyohara J, Asai T, Welch MJ, Adams SG, Saji H, Yonekura Y, Fujibayashi Y. Basic characterization of ^{64}Cu-ATSM as a radiotherapy agent. *Nucl Med Biol* 2005;32:21-28.
33. Pavlik C, Biswal NC, Gaenzler FC, Morton MD, Kuhn LT, Claffey KP, Zhu Q, Smith MB. Synthesis and fluorescent characteristics of imidazole–indocyanine green conjugates. *Dyes Pigments* 2011;89:9-15.
34. Xu Y, Zanganeh S, Mohammad I, Aguirre A, Wang T, Yang Y, Kuhn L, Smith MB, Zhu Q. Targeting tumor hypoxia with 2-nitroimidazole-indocyanine green dye conjugates. *J Biomed Optics* 2013;18:066009.
35. Okuda K, Okabe Y, Kadonosono T, Ueno T, Youssif BG, Kizaka-Kondoh S, Nagasawa H. 2-Nitroimidazole-tricarbocyanine conjugate as a near-infrared fluorescent probe for in vivo imaging of tumor hypoxia. *Bioconjug Chem* 2012;23:324-329.
36. Youssif BG, Okuda K, Kadonosono T, Salem OI, Hayallah AA, Hussein MA, Kizaka-Kondoh S, Nagasawa H. Development of a hypoxia-selective near-infrared fluorescent probe for non-invasive tumor imaging. *Chem*

Pharm Bull 2012;60:402-407.

37. Stanford CL. Synthesis of half-loaded nitroimidazole indocyanine green dyes attached to carbon nanotubes. *Master Science Thesis*. 2012.
38. Biswal NC, Pavlik C, Smith MB, Aguirre A, Xu Y, Zanganeh S, Kuhn LT, Claffey KP, Zhu Q. Imaging tumor hypoxia by near-infrared fluorescence tomography. *J Biomed Optics* 2011;16:066009--8.
39. Kiyose K, Hanaoka K, Oushiki D, Nakamura T, Kajimura M, Suematsu M, Nishimatsu H, Yamane T, Terai T, Hirata Y, Nagano T. Hypoxia-sensitive fluorescent probes for in vivo real-time fluorescence imaging of acute ischemia. *J Am Chem Soc* 2010;132:15846-14848.
40. Piao W, Tsuda S, Tanaka Y, Maeda S, Liu F, Takahashi S, Kushida Y, Komatsu T, Ueno T, Terai T, Nakazawa T, Uchiyama M, Morokuma K, Nagano T, Hanaoka K. Development of azo-based fluorescent probes to detect different levels of hypoxia. *Angew Chem Int Ed* 2013;52:13028-13032.
41. Zhang S, Hosaka M, Yoshihara T, Negishi K, Iida Y, Tobita S, Takeuchi T. Phosphorescent light–emitting iridium complexes serve as a hypoxia-sensing probe for tumor imaging in living animals. *Ca Res* 2010;70:4490-4498.
42. Napp J, Behnke T, Fischer L, Würth C, Wottawa M, Katschinski DrM, Alves F, Resch-Genger U, Schäferling M. Targeted luminescent near-infrared polymer-nanoprobes for in vivo imaging of tumor hypoxia. *Anal Chem* 2011;83:9039-9046.
43. Raleigh J, Chou S, Arteel G, and Horsman M. Comparisons among pimonidazole binding, oxygen electrode measurements, and radiation response in C3H mouse tumors. *Radiat Res* 1999;151:580-589.
44. Samoszuk MK, Walter J, and Mechetner E. Improved immunohistochemical method for detecting hypoxia gradients in mouse tissues and tumors. *J Histochem Cytochem* 2004;52:837-839.
45. Samoszuk M, Corwin MA. Mast cell inhibitor cromolyn increases blood clotting and hypoxia in murine breast cancer. *Int J Ca* 2003;107:159-163.
46. Bache M, Kappler M, Said HM, Staab A, Vordermark D. Detection and specific targeting of hypoxic regions within solid tumors: current preclinical and clinical strategies. *Curr Med Chem* 2008;15:322-338.
47. Gibbs SL. Near infrared fluorescence for image-guided surgery. *Quan Imaging Med Surg* 2012;2:177-187.
48. Baker KJ. Binding of sulfobromophthalein (BSP) sodium and indocyanine green (ICG) by plasma alpha-1 lipoproteins. Proc Soc Exp Bio Med 1966;122:957-963.
49. Landsman M, Kwant G, Mook G, Zijlstra W. Light-absorbing properties, stability, and spectral stabilization of indocyanine green. *J Appl Physiol* 1976;40:575-583.
50. Krohn KA, Link JM, Mason RP. Molecular imaging of hypoxia. *J Nucl Med* 2008;49:129S-48S.
51. Kizaka-Kondoh S, Inoue M, Harada H, and Hiraoka M. Tumor hypoxia: a target for selective cancer therapy. *Ca Sci* 2003;94:1021-1028.
52. Hoigebazar L, Jeong JM, Hong MK, Kim YJ, Lee JY, Shetty D, Lee YS, Lee DS, Chung JK, Lee MC. Synthesis of ^{68}Ga-labeled DOTA-nitroimidazole derivatives and their feasibilities as hypoxia imaging PET tracers. Bioorg *Med Chem* 2011;19:2176-2181.
53. Kelada OJ, Carlson DJ. Molecular imaging of tumor hypoxia with positron emission tomography. *Radiat Res* 2014;181:335-349.
54. Ntziachristos V. Fluorescence molecular imaging. *Ann Rev Biomed Eng* 2006;8:1-33.
55. Zhang XF, Zhang J, Liu L. Fluorescence properties of twenty fluorescein derivatives: lifetime, quantum yield, absorption and emission spectra. *J Fluores* 2014;24:819-826.
56. Savarese M, Aliberti A, De Santo I, Battista E, Causa F, Netti PA, Rega N. Fluorescence lifetimes and quantum yields of rhodamine derivatives: New insights from theory and experiment. *J Phys Chem* 2012;116:7491-7497.